RSC Advances

Suppression of photocatalysis and long-lasting luminescence in $ZnGa_2O_4$ by Cr^{3+} doping

Lei Li, Yin-hai Wang,* Hong Li, Hai-ju Huang, Hui Zhao

Abstract

$ZnGa_2O_4$ powder, synthesized by a solid state method, exhibit efficient photocatalytic activity for rhodamine B (RhB) degradation under mercury lamp illumination. However, the photocatalytic activity of $ZnGa_2O_4$ was highly suppressed due to Cr^{3+} ions doping. We discussed the mechanism of photocatalysis based on the photoluminescence properties of $ZnGa_2O_4$ and $ZnGa_2O_4:Cr^{3+}$, and the blue fluorescence lifetimes of host $ZnGa_2O_4$ with different Cr^{3+} concentrations were also measured. The results indicated that Cr^{3+} ions doping are act as recombination centers, which can highly reduce the amount and lifetime of the electron-hole pairs and thus reduce the photocatalytic activity of $ZnGa_2O_4$. The thermoluminescence (TL) curves of $ZnGa_2O_4$ and $ZnGa_2O_4:Cr^{3+}$ showed that the amount of trapped electrons/holes in $ZnGa_2O_4$ is almost seven times higher than that of $ZnGa_2O_4:Cr^{3+}$. The suppressed long-lasting luminescence intensity and photocatalytic activity of $ZnGa_2O_4:Cr^{3+}$ were supposed to come from the decrease of trapped electrons/holes and shortened lifetime of the electron-hole pairs. Possible mechanisms of long-lasting luminescence and photocatalysis of $ZnGa_2O_4$ coupled with photoluminescence mechanisms of $ZnGa_2O_4:Cr^{3+}$ were also proposed.

Introduction

Long-lasting luminescence is an optical phenomenon whereby luminescence can remain visible for a long time (seconds to hours) after the excitation has stopped.[1-3] These materials have long been of great interest and are drawing more and more attention in recent years due to the great potential applications in many fields, such as emergency signage, traffic signs and in vivo bio-imaging.[4]

As a kind of wide band gap (4.5 ev) semiconductor, $ZnGa_2O_4$ phosphor has attracted enormous attentions due to its many possible applications for field emission displays and electroluminescent devices due to its chemically and mechanically stable structure which may sustain under harsh environments.[5, 6] $ZnGa_2O_4$ phosphor has a cubic normal AB_2O_4 spinel crystal structure with Fd3m space group[7] in which Zn^{2+} ions surrounded by 4 oxygens occupy the tetrahedral A sites and Ga^{3+} surrounded by

6 oxygens the octahedral B sites. With this spinel structure, $ZnGa_2O_4$ can be described in terms of a close packed cubic arrangement of 32 oxygen anions. There are 64 tetrahedral sites and 32 octahedral sites in which only a half of the octahedral gaps and one-eighth of the tetrahedral gaps are filled with cations.[8] So $ZnGa_2O_4$ is an ideal host lattice for doping with transition metals or rare earth elements to form the luminescence center. $ZnGa_2O_4$ shows blue emission attributed to self-activated centers when undoped,[9, 10] intense green emission when doped with Mn^{2+} and near-infrared (NIR) luminescence with Cr^{3+} doping.[11, 12]

Recently, $ZnGa_2O_4$ is also reported to exhibits excellent performance in water splitting[13] and air purification[14, 15] due to its high photocatalytic activity. It is considered that the highly dispersed LUMO (bottom of conduction band), composed of hybridized orbitals of Ga 4s4p and Zn 4s4p atomic orbitals,[16, 17] promotes the mobility of photo-generated electrons and benefits the high photocatalytic activity of $ZnGa_2O_4$.[18] In the work of Sun *et al.*,[19] $ZnGa_2O_4$ synthesized by rapid microwave hydrothermal method exhibits efficient photocatalytic activities even higher than that of commercial TiO_2 P25. Nowadays, inspired by the methods to improve the photocatalytic activities of TiO_2, many approaches are proposed to improve the photocatalytic activity of $ZnGa_2O_4$ (controlling morphology, calcining temperature, PH value, trace element doping, chemical ratio).[18-25] In the literatures about photocatalysis of TiO_2, Cr^{3+} ions doping has been of interest in the study of visible–light-induced photocatalytic activity due to its extension of the spectral response into the visible range. Whereas there are many articles about Cr^{3+} ions doped TiO_2,[26-28] the photocatalytic activity of $ZnGa_2O_4$:Cr^{3+} has never been discussed, even though Cr^{3+} doped $ZnGa_2O_4$ can increase the disorder of spinel structure of $ZnGa_2O_4$ and thus induce more defects which may in favor of the photocatalytic activity.

Here $ZnGa_2O_4$ host and Cr^{3+} doped $ZnGa_2O_4$ samples are prepared by traditional high temperature solid state method. Photocatalytic activity test shows that photo-degradation efficiency of $ZnGa_2O_4$ is highly suppressed via doping with Cr^{3+}, which is unexpected and triggered us to discuss the mechanism of photocatalysis of $ZnGa_2O_4$:Cr^{3+} in detail. It is generally considered that peroxide ($\cdot O_2^-$) and hydroxyl radical ($\cdot OH$), generated by the reaction of the photo-generated electrons with O_2 and H_2O, are highly responsible for photocatalytic degradation of pollutants and can oxidize organic pollutants into CO_2 and H_2O.[22] So the photo-generated electrons play important roles in photocatalysis, the amount and lifetime of photo-generated

electrons can highly influence the photocatalytic activity of photocatalyst. It is known that the photo-generated electrons and holes recombine fast at recombination centers after the stoppage of excitation. The recombination rate could be decreased by the presence of ions acting as electron or hole traps which can maintain the photo-generated electrons/holes for a longer period and thus in favor of increasing photocatalytic activity. On the other hand, the recombination rate could be increased by the presence of ions acting as recombination centers such as defects or multiphases,[29] which can reduce the amount and lifetime of electron-hole pairs. Therefore, the relative efficiency of a metal ion dopant depends on whether it serves as a mediator of interfacial charge transfer or as a recombination center.[30] It is well known that the photoluminescence results from recombination of photo-generated electrons and holes, and the recombination rate determines the luminescence intensity. Therefore, there is a competitive mechanism between luminescence intensity and photocatalytic activity. That is to say, the lower the recombination rate of photo-generated electrons and holes, the lower the photoluminescence intensity, and the higher the photocatalytic activity. The suppression of photocatalytic activity in $ZnGa_2O_4$ by Cr^{3+} doping can be investigated based on the luminescence properties of $ZnGa_2O_4:Cr^{3+}$. It is promising to discuss the photocatalytic activity accompany with luminescence properties, and a promising approach via controlling the luminescence properties can be proposed to develop the photocatalytic activity of photocatalysts.

Experimental
Materials

Chemical reagents ZnO (99%), Ga_2O_3 (99.99%), Cr_2O_3 (99%) were used as starting materials, chromium is nominally doped with 0.1%, 0.3%, 0.5%, 0.7%, 1.0% and 1.5% mol relative to gallium. Appropriate amount of starting materials with different stoichiometric ratios were mixed and carefully pestled in an agate mortar for about 1 h to make sure it is homogeneous, then the mixed powders were moved into a corundum crucible and calcined at 1300 ^{o}C for 4 h in the air atmosphere. When the samples were cooled to room temperature, pestle them again respectively with the agate mortar.

Characterization

The crystal structure of the powder phosphors were analyzed using a X-ray diffractometer at room temperature using Cu K_α (λ=1.5418Å) irradiation operating at 36 kV and 20 mA. Data were collected between 10° and 70° (2θ) at room temperature with a 0.02^o step size. The surface morphologies were observed using a Scanning Electron Microscopy (SEM, S-3400N-II, Japan). The particle sizes of the powder phosphors were measured by Laser Particle Size Analyzer (JL-1197). The excitation and emission spectra, long-lasting luminescence decay curves and fluorescence decay curves were obtained at room temperature using a Hitachi F-7000 fluorescence spectrophotometer. An FJ27A1 TL dosimeter was used to measure TL curves at the heating rate of 1^oC/s after the samples were exposed to radiation from a UV lamp for 5 min and placed in dark room for 3 min.

Photocatalytic activity test

The photocatalytic activities were characterized by the photo-degradation of RhB. A 500 W mercury lamp with 5 A operating current was used as light source, the mercury lamp was positioned in a cylindrical Pyrex vessel and cooled by circulating water to control the reaction temperature at about 27 ^{o}C when irradiation was performed. As-prepared $ZnGa_2O_4$ and $ZnGa_2O_4$:Cr^{3+} particles (0.01 g) were firstly dispersed in two glass tubes with 40 ml RhB solution (4×10^{-5} mol/l) respectively, another glass tube only with 40 ml RhB solution was prepared as the blank solution. Then the suspensions were stirred in the dark for 30 min to achieve an adsorption/desorption equilibrium between the photocatalyst and RhB solution, during which vigorous magnetic stirring was maintained to keep $ZnGa_2O_4$ and $ZnGa_2O_4$:Cr^{3+} particles suspended in the RhB solution. Then 5 ml suspensions were added into centrifuge tubes and centrifuged for 3 min at 3000 r/min to eliminate the solid particles. The clear supernatant were used to measure the changes of the RhB concentration (the solid particles and clear supernatant were poured back into glass tubes respectively to make sure there is always a comparable amount $ZnGa_2O_4$ and $ZnGa_2O_4$:Cr^{3+} in the RhB solution). The RhB concentration was monitored at the maximum absorbance wavelength of 553 nm. The percentage of degradation was recorded as C/C_0, in which C is the absorbance of RhB solution at certain irradiated time intervals (10 min) and C_0 is the absorbance of the initial RhB solution. The blank solution was also tested under same experimental conditions for comparison.

Results and discussion

Fig. 1 shows the X-ray diffraction (XRD) patterns of $ZnGa_2O_4$ and $ZnGa_2O_4:Cr^{3+}$ calcined at 1300 ^{o}C for 4 h. All the peaks are assigned to $ZnGa_2O_4$ spinel phase (JCPDS No. 38-1240) and no characteristic peaks of the dopants have been observed. Nine distinctive peaks match well with the (111), (220), (311), (222), (400), (422), (511), (440), and (531) crystal planes of $ZnGa_2O_4$, respectively. The result indicates that the pure spinel phase of $ZnGa_2O_4$ is formed in the samples to be investigated. Therefore, the doping of 0.5% mol transition metal ion chromium relative to gallium has no significant influence on the crystal structure of $ZnGa_2O_4$. The morphologies of as-synthesized $ZnGa_2O_4$ and $ZnGa_2O_4:Cr^{3+}$ were demonstrated in the SEM images (shown in Fig. 2). As shown in Fig. 2, as-prepared $ZnGa_2O_4$ and $ZnGa_2O_4:Cr^{3+}$ samples show same irregular shape. Particles are partly agglomerated, and the particles of $ZnGa_2O_4:Cr^{3+}$ are agglomerated more seriously. The actual particle sizes of $ZnGa_2O_4$ and $ZnGa_2O_4:Cr^{3+}$ are about 0.75 um and 0.70 um, respectively. Fig. 3 shows the distribution of particle sizes of the powder phosphors. As shown in Fig. 3, the average particle sizes of $ZnGa_2O_4$ and $ZnGa_2O_4:Cr^{3+}$ are about 0.78 um and 0.80 um, respectively. The results are consistent with the actual particle sizes and agglomeration shown in Fig. 2. The results about crystal structure, morphology, particle size and size distribution indicated that $ZnGa_2O_4$ and $ZnGa_2O_4:Cr^{3+}$ possess almost the same surface areas and same amount of $ZnGa_2O_4$ and $ZnGa_2O_4:Cr^{3+}$ powders are comparable in photocatalytic reaction.
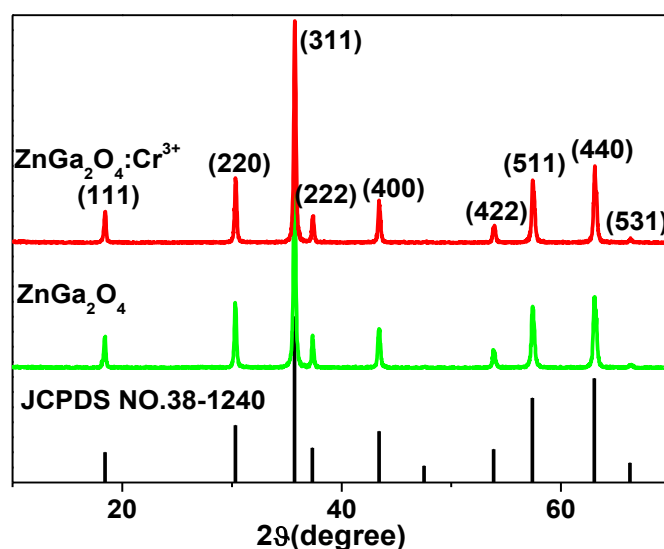
Fig. 1 XRD patterns of $ZnGa_2O_4$ and $ZnGa_2O_4:Cr^{3+}$.
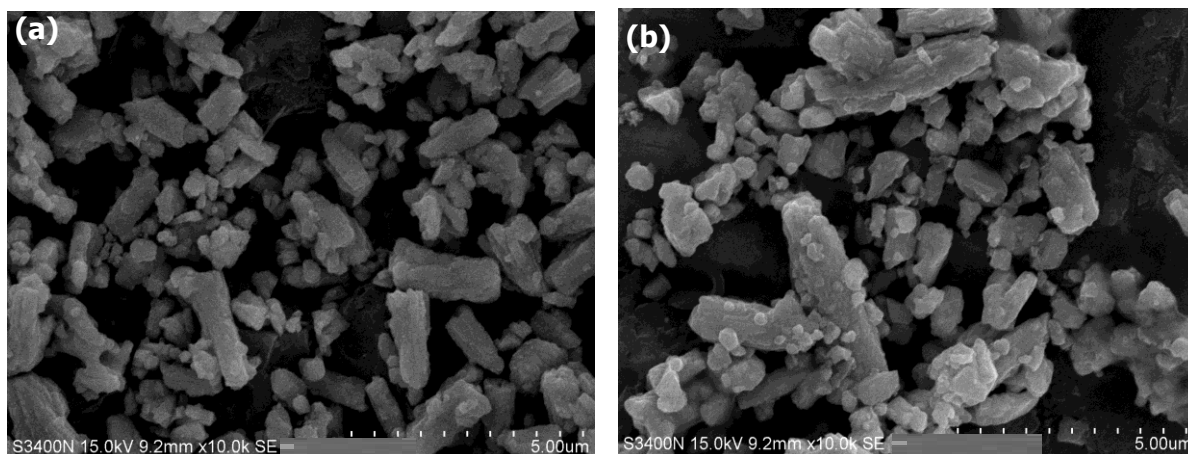
Fig. 2 The morphologies of the as-synthesized $ZnGa_2O_4$ (a) and $ZnGa_2O_4:Cr^{3+}$ (b).
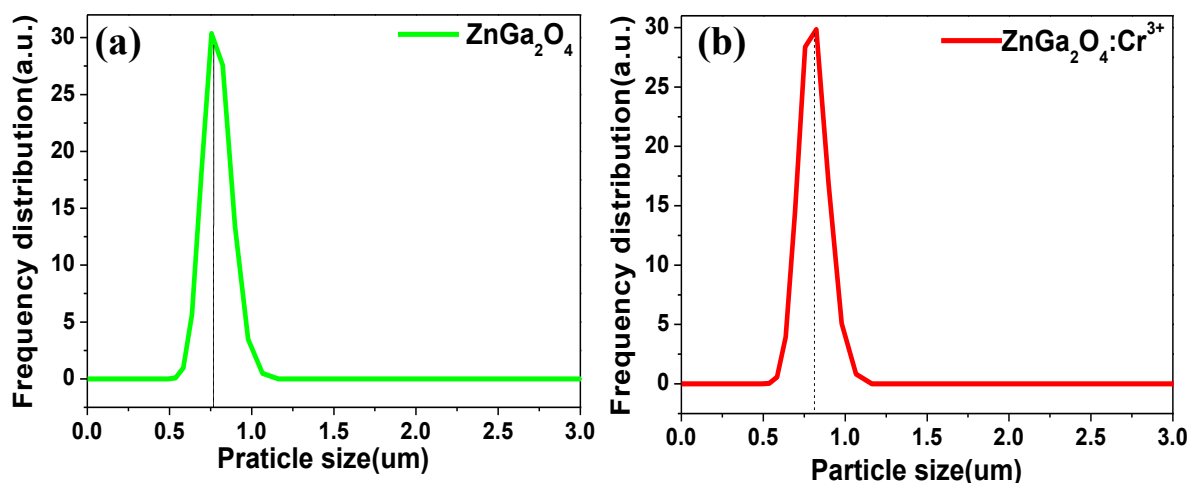
Fig. 3 Frequency distribution of particle sizes of $ZnGa_2O_4$ (a) and $ZnGa_2O_4:Cr^{3+}$ (b).

The photo-degradation of RhB were measured as a function of irradiation time as shown in Fig. 4. The degradation rate of RhB under irradiation was very slow when no photocatalyst was added (blank in Fig. 4). Also, the photocatalytic activity of $ZnGa_2O_4:Cr^{3+}$ can be ignored. On the contrary, the RhB concentration underwent an obvious decline after 110 min irradiation in presence of $ZnGa_2O_4$ with 60% RhB degradation.
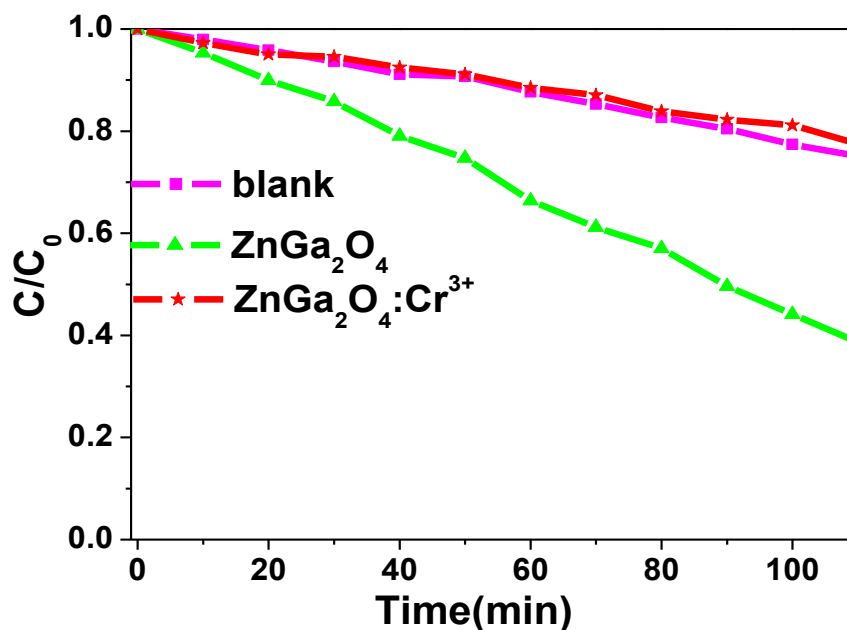
Fig. 4 Photocatalytic activity of $ZnGa_2O_4$ and $ZnGa_2O_4:Cr^{3+}$ for degradation of RhB under mercury lamp, the percentage of degradation is recorded at 10 min irradiated time intervals.

An appropriate electronic structure is essential for the photocatalytic activity. Recently, Sun *et al.*[19] reported that the band-edge positions of the conduction and valence bands (E_{CB} and E_{VB}, respectively) can be calculated by the following empirical equations:[31]

$$E_{CB} = -\chi + 1/2E_g \tag{1}$$
$$E_{VB} = -\chi - 1/2E_g \tag{2}$$

where E_g is the band gap energy and χ is the Mulliken electronegativity of a pristine semiconductor. This method has achieved success in calculating band positions and photoelectric thresholds for many materials.[32–34] For $ZnGa_2O_4$ catalyst, using the empirical equations described above, E_{VB} was determined to be 3.35 V versus normal hydrogen electrode (NHE), more positive than that of $E(•OH/OH^-)$ (2.38 V, NHE) and E_{CB} was -1.45 V (NHE), more negative than that of $E(O_2/•O_2^-)$ (-0.33 V, NHE).[35] The higher valence band position and lower conduction band position means •OH can be generated by UV-irradiated $ZnGa_2O_4$ in RhB solution, exhibiting photocatalytic activity. From Fig. 4, it is obvious that the photo-degradation of RhB with $ZnGa_2O_4$ is highly suppressed when doped with Cr^{3+}. As mentioned above, there is a competitive mechanism between luminescence intensity and photocatalytic activity, the reason why doping Cr^{3+} could suppress the photocatalytic activity of $ZnGa_2O_4$ will be discussed in detail mainly on the basis of luminescence properties of $ZnGa_2O_4:Cr^{3+}$.

Fig. 5 shows the emission spectra of $ZnGa_2O_4$ and $ZnGa_2O_4:Cr^{3+}$ at room temperature under the excitation with the wavelength of 254 nm. The self-activated photoluminescence of $ZnGa_2O_4$ host exhibit a broad-band emission peaking at 340 nm, a narrow-band emission with the maximum emission at 505 nm, and a weak band emission peaking at 680 nm under 254 nm excitation. The emission band at 505 nm (^2E_A-$^4A_2$) is likely due to the electrons and holes recombination between the native defects (oxygen defect, Zinc defect, and gallium-oxygen vacancy pair).[36-38] The emission band at 340 nm is similar to the band at 360 nm reported by Kim *et al.*,[39, 40] which is the blueshift behavior of emission band from 430 nm to 340 nm. The blueshift behavior is resulted from the oxygen vacancy (V_O*) defects which distort the symmetry of the O_h site, leading to the Ga-O transition emission of regular octahedral sites at 430 nm shift to 340 nm which originated from Ga-O transition emission of distorted octahedral sites.[41, 42] Also, 698 nm emission accompanying the 340 nm emission is identified as the transition from the V_O* state to the O^{2-} state.[40] In contrast, $ZnGa_2O_4:Cr^{3+}$ gave an intense NIR emission band at 698 nm due to the ^2E-$^4A_2$ transition of distorted Cr^{3+} ions in $ZnGa_2O_4$.[43] The host emission at 505 nm is highly suppressed after doping Cr^{3+} into $ZnGa_2O_4$ due to an effective nonradiative energy transfer between the host emission and the absorption of Cr^{3+} ($^4A_2$-$^4T_1$ (te^2), $^4A_2$-$^4T_1$ (t^2e) and $^4A_2$-$^4T_2$ transition) resulting from their large spectral overlap.[43] The result is similar to the energy transfer between the blue emission of $ZnGa_2O_4$ host and the absorption of Cr^{3+}.[43, 44] The excitation spectra of the $ZnGa_2O_4:Cr^{3+}$ have three main bands (in the inset of Fig. 5), the excitation peak at 260 nm results from the combination of the $ZnGa_2O_4$ host excitation band and the O-Cr charge transfer band.[43] The other two bands at 410 nm ($^4A_2$-$^4T_1$ (te^2) transition) and 550 nm ($^4A_2$-$^4T_2$ transition) originate from the 3d intrashell transitions of Cr^{3+}.[45]

As we mentioned above, the recombination rate of photo-generated electrons and holes determines the photoluminescence intensity. Hence, the intense emission intensity of $ZnGa_2O_4:Cr^{3+}$ at 698 nm compared with that of $ZnGa_2O_4$ at 505 nm indicating that Cr^{3+} ions doping may acted as recombination centers. The entrained recombination centers, which can highly reduce the amount and lifetime of photo-generated electron-hole pairs, could be the cause of suppressed photocatalytic activity in $ZnGa_2O_4:Cr^{3+}$.
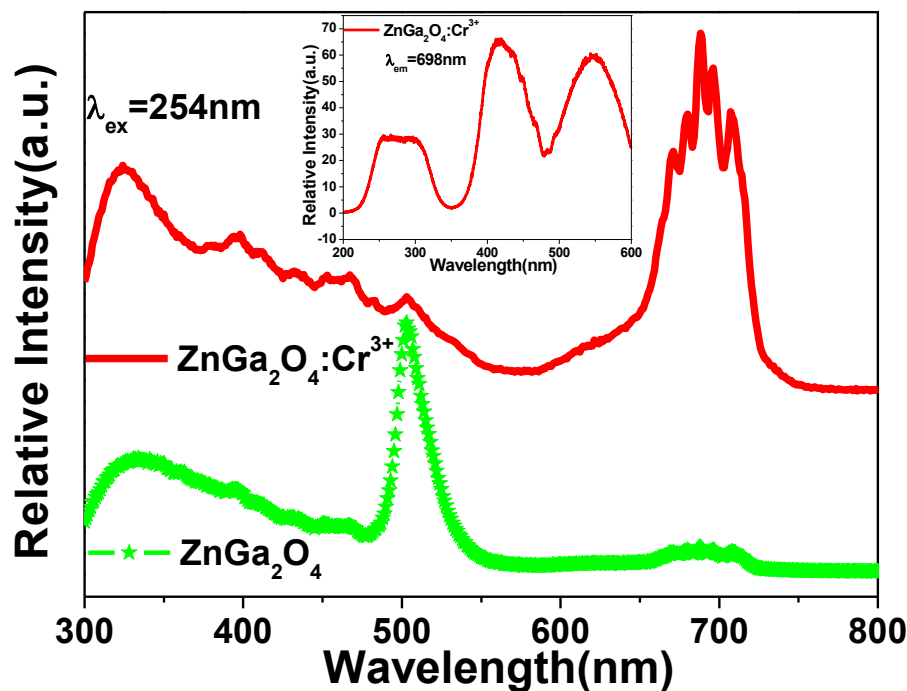
Fig. 5 Emission spectra of $ZnGa_2O_4$ and $ZnGa_2O_4$:Cr^{3+} at room temperature under the excitation with the wavelength of 254 nm. The inset shows the excitation spectra of $ZnGa_2O_4$:Cr^{3+} monitored at 689 nm.

In order to prove that Cr^{3+} ions are acts as recombination centers, the blue fluorescence lifetimes (at 505 nm) of $ZnGa_2O_4$ were measured with different Cr^{3+} doping concentrations (x=0.0%, 0.1%, 0.3%, 0.5%, 0.7%, 1.0%, 1.5%). As showed in Fig. 6, those fluorescence decay curves can be fitted by a single exponential function and the fitting results of the lifetimes are shown in the inset. It is clearly observed that the lifetimes of $ZnGa_2O_4$ at 505 nm become shorter with the increase of the Cr^{3+} concentration as the result of energy transfer from $ZnGa_2O_4$ to Cr^{3+}.[46] The fluorescence lifetime reflects the average residence time of photo-generated electrons in the excited state. The shortened fluorescence lifetime of $ZnGa_2O_4$ means that the energy transfer become quicker with the increase of the Cr^{3+} concentration, and the average residence time of photo-generated electrons in the excited state shortened faster. Therefore, there are more channels are formed benefiting the recombination of electrons and holes to transfer energy to Cr^{3+}, Cr^{3+} ions doping are acts as recombination centers in $ZnGa_2O_4$ which accelerating the recombination of electrons and holes.
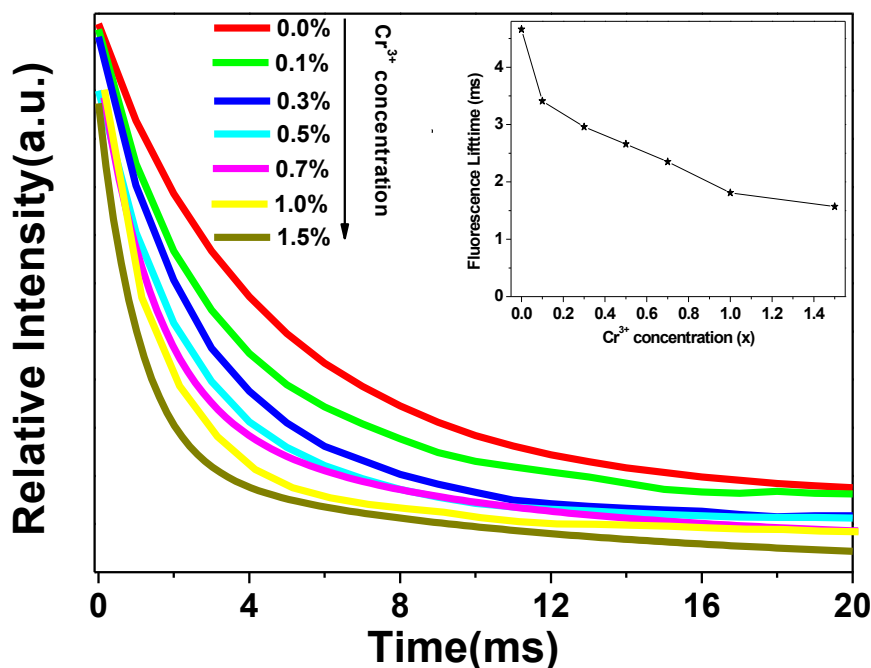
Fig. 6 The fluorescence decay curves of $ZnGa_2O_4$ (505 nm emission) with different Cr^{3+} doping concentration (x=0.0%, 0.1%, 0.3%, 0.5%, 0.7%, 1.0%, 1.5%). The inset shows the fitting results of the lifetimes.

As it is generally accepted, long-lasting luminescence is a phenomenon whereby luminescence can last for hours after the stoppage of the excitation. The long-lasting luminescence of the phosphors is generated by the recombination of trapped electrons and holes which are released slowly through thermal motion after the stoppage of excitation. We measured the afterglow decay curves of $ZnGa_2O_4$ and $ZnGa_2O_4:Cr^{3+}$ phosphors monitored at 505 nm and 698 nm after 5 min irradiation with a 254 nm UV lamp, respectively. As can be seen from Fig. 7, as-prepared samples exhibit similar decay processes which contain a rapid decay at beginning and a slow decay process afterward.[47, 48] In our study, the decay curves can be well fitted by a double exponential equation and as follows: $I = I_1 \exp(\frac{-t}{\tau_1}) + I_2 \exp(\frac{-t}{\tau_2})$

where t is the decay time; I(t) represents the phosphorescent intensity at the t time; I_1 and I_2 are constants which depend on the rapid and slow initial luminescent intensity at t = 0, while τ_1 and τ_2 are decay constants which decide the rate for the rapid and slow exponential decay components, respectively. The parameters τ_1 and τ_2 are calculated and the fitting results are shown in Table 1. These parameters indicate that $ZnGa_2O_4$ exhibits better long-lasting luminescence properties than that of $ZnGa_2O_4:Cr^{3+}$. After 5 min decay time, the long-lasting luminescence intensity of

ZnGa$_2$O$_4$ is still high. The inset of Fig. 7 displays the afterglow brightness of ZnGa$_2$O$_4$ and ZnGa$_2$O$_4$:Cr^{3+} recorded at different decay times after irradiation with the wavelength of 254 nm for 5 min. The results about long-lasting luminescence are consistent with that of photocatalytic performance in Fig. 4. We think that Cr^{3+} ions doping are act as recombination centers but not trap centers and the suppression of long-lasting luminescence intensity of ZnGa$_2$O$_4$:Cr^{3+} comes from less trapped electrons/holes in ZnGa$_2$O$_4$:Cr^{3+}.
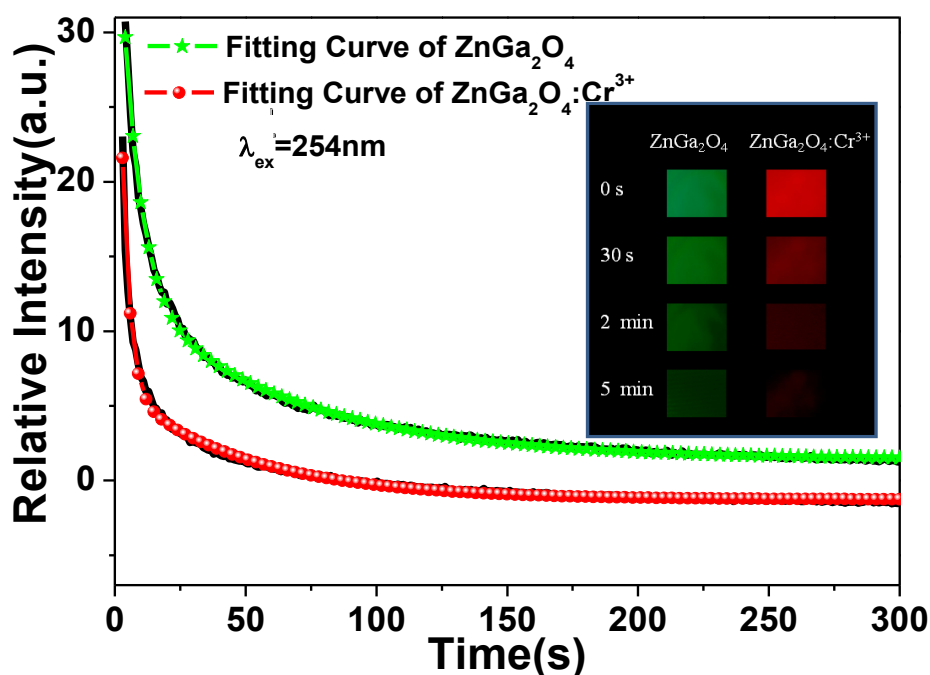
Fig. 7 Afterglow decay curves of ZnGa$_2$O$_4$ and ZnGa$_2$O$_4$:Cr^{3+} phosphors monitored at 505 nm and 698 nm after 5 min irradiation with a 254 nm UV lamp, respectively. The fitting curves are shown as green line with star and red line with circle, respectively. The inset shows the digital photos of afterglow brightness of ZnGa$_2$O$_4$ and ZnGa$_2$O$_4$:Cr^{3+} recorded at different decay times after irradiation with the wavelength of 254 nm for 5 min.

Table: 1 The fitting results of decay curves.

Samples	A$_1$/(a.u.)	τ_1/(s)	A$_2$/(a.u.)	τ_2/(s)
ZnGa$_2$O$_4$	31.00	6.96	11.49	63.24
ZnGa$_2$O$_4$:Cr^{3+}	20.77	3.00	6.93	68.77

As the TL curve can reflect the trapping property of defects, as well as the relevance of the long-lasting luminescence and the trap energy levels. We measured the TL curves of ZnGa$_2$O$_4$ and ZnGa$_2$O$_4$:Cr^{3+} at the region of 40 ^{o}C-260 ^{o}C. In Fig. 8, under same experimental condition (same volume of the samples are irradiated for 5

min by UV lamp and then placed in dark room for 3min before the measurement), the maximum TL intensity of $ZnGa_2O_4$ is almost seven times higher than that of $ZnGa_2O_4:Cr^{3+}$ under thermal disturbance. That means after the stoppage of irradiation by UV lamp, the amount of trapped electrons/holes in $ZnGa_2O_4$ is almost seven times higher than that of $ZnGa_2O_4:Cr^{3+}$. When heating, those captured electrons and holes will be released from traps and recombine with each other in the form of TL. Less trapped electrons/holes means less trap centers, the results of TL curves confirmed that decreased trap centers are formed in $ZnGa_2O_4$ when doped with Cr^{3+}.
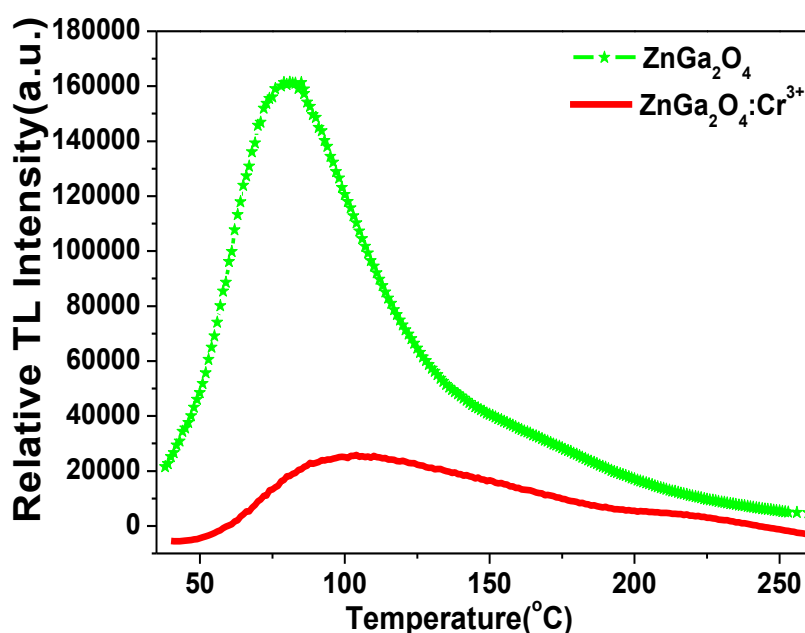
Fig. 8 TL curves of $ZnGa_2O_4$ and $ZnGa_2O_4:Cr^{3+}$ at the region of 40^oC-260^oC. The sample was irradiated for 5 min by UV lamp and then placed in dark room for 3min before the measurement.

In $ZnGa_2O_4$ lots of photo-generated electrons and holes occurred with a irradiation energy that is larger than the band gap energy of $ZnGa_2O_4$,[49] one part of photo-generated electrons and holes recombine at recombination centers quickly to release energy in the form of photoluminescence, the other part can be trapped by lattice defects, impurities, or co-dopants which act as traps in the material.[50, 51] The trapped photo-generated electrons/holes can delay the recombination of electrons and holes, which promoting the separation of electrons and holes and enhancing charge transfer, thus improving the photocatalytic activity effectively. After stopping the radiation and with the thermal disturbance at proper temperature, these trapped electrons and holes will be released from the traps and then recombine with each other, followed by the emission as long-lasting luminescence. Hence, photocatalysis and

long-lasting luminescence are significantly associated. That is to say, the more trapped electrons and holes, the stronger long-lasting luminescence intensity, and the higher photocatalytic activity will be.

Based on the discussion above, a possible schematic illustration of long-lasting luminescence and photocatalysis for $ZnGa_2O_4$ was proposed and depicted in Fig. 9a. Upon 254 nm UV excitation, the incident photons are absorbed by $ZnGa_2O_4$ host and the electrons are promoted from the valence band of $ZnGa_2O_4$ to the conduction band (progress (1)). Most of the electrons will be transferred via the lattice directly to the luminescence centers (progress (2)), followed by the emission ^2E_A-$^4A_2$ and ^2E_B-$^4A_2$ as photoluminescence (progress (3) and (4)), a part of the excitation energy associated with the excited free electrons are captured by native defects via nonradiative relaxation (progress (5)). After UV irradiation is stopped, with the thermal disturbance at proper temperature, these carriers will be released from the traps and transferred via the host to the luminescence center (progress (6)) and then recombine with the opposite charge, followed by the ^2E_A-$^4A_2$ emission as long-lasting luminescence. When excited free electrons are captured by electron traps, the photo-generated electrons and holes can be effectively separated, which could prevent the recombination of electrons and holes, leading to a longer lifetime of the photo-generated electrons and holes. Then the O_2 near the interface of photocatalyst/liquid could be reduced to the superoxide radical anion $\bullet O_2^-$ and hydrogen peroxide H_2O_2 (Eqs. (3) and (4)) by the photoelectrons. The $\bullet O_2^-$ and H_2O_2 can further interact to produce hydroxyl radical $\bullet OH$ (Eq. (6)), which is able to decompose most organic pollutants in water as a powerful oxidizing species.[52]

$$e^- + O_2 \rightarrow \cdot O_2^- \tag{3}$$

$$O_2 + 2H^+ + 2e^- \rightarrow H_2O_2 \tag{4}$$

$$H_2O_2 + e^- \rightarrow \cdot OH + OH^- \tag{5}$$

$$H_2O_2 + \cdot O_2^- \rightarrow \cdot OH + OH^- + O_2 \tag{6}$$

$$H_2O_2 \rightarrow 2 \cdot OH \tag{7}$$
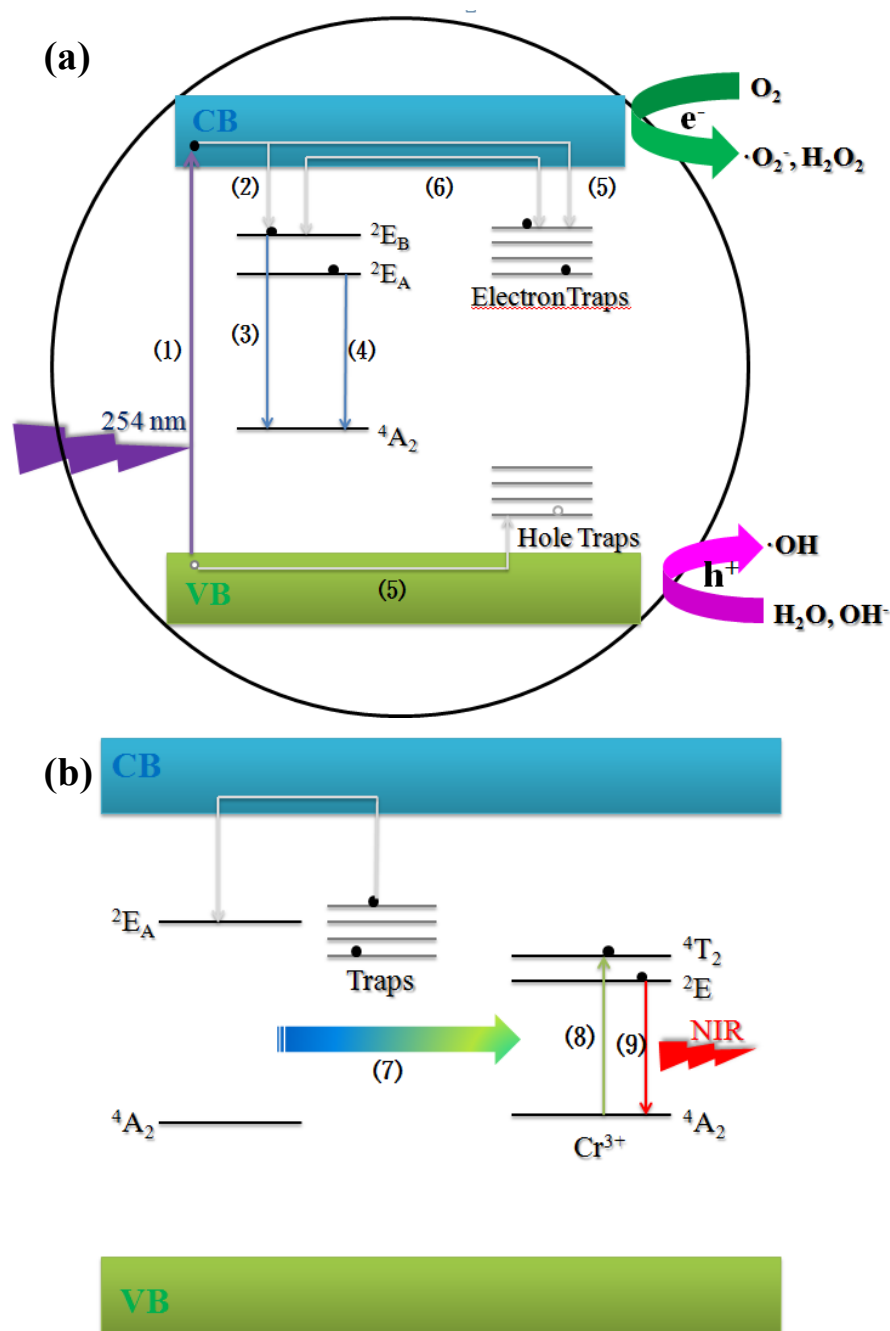
Fig. 9 (a) Schematic illustration of long-lasting luminescence and photocatalysis of $ZnGa_2O_4$. (b) Mechanism illustration of the persistent energy transfer between $ZnGa_2O_4$ host and Cr^{3+} ion.

Fig. 9b presented a possible mechanism of photoluminescence for $ZnGa_2O_4:Cr^{3+}$. After UV irradiation is stopped, these photo-generated electrons and holes captured by traps can be released slowly through thermal motion. Instead of recombining with the opposite charge to produce the ^2E_A-$^4A_2$ emission as long-lasting luminescence, the energy associated with electrons of the host is persistently transferred to the Cr^{3+} ion slowly via an effective nonradiative energy transfer (progress (7)).[53] The persistent energy transfer leads to the promotion of the 3d electrons of Cr^{3+} from ground-state

(^{4}A$_2$) to the excited-states ^{4}T$_2$ (progress (8)). The transitions between ^{4}T$_2$ and ^{2}E is just nonradiative reactions. Then ^{2}E-^{4}A$_2$ transition gave a NIR emission band at 698 nm and produce the persistent luminescence (progress (9)) which comes from the persistent energy transfer from the host.

Conclusions

In summary, ZnGa$_2$O$_4$ presents high photocatalytic activity to degrade RhB and excellent long-lasting luminescence properties under UV irradiation. The favorable edge position of E$_{CB}$ and E$_{VB}$ results in the strong redox ability of ZnGa$_2$O$_4$. When doped with Cr^{3+}, it's photocatalytic activity and long-lasting luminescence intensity are highly suppressed, and there is an effective persistent energy transfer between the host emission and the absorption of Cr^{3+} resulting the NIR long-lasting luminescence at 698 nm. The surface areas of as-synthesized ZnGa$_2$O$_4$ and ZnGa$_2$O$_4$:Cr^{3+} samples are almost same and the average particle sizes are about 0.78 um and 0.80 um, respectively. The results indicated that same amount of ZnGa$_2$O$_4$ and ZnGa$_2$O$_4$:Cr^{3+} powders are comparable in photocatalytic reaction. From luminescence properties, fluorescence decay curves and TL curves, there comes a conclusion that Cr^{3+} ions doping are act as recombination centers but not trap centers and the amount of trapped electrons/holes in ZnGa$_2$O$_4$ is almost seven times higher than that of ZnGa$_2$O$_4$:Cr^{3+}. Therefore, it is proposed that the suppressed photocatalytic activity and long-lasting luminescence intensity in ZnGa$_2$O$_4$:Cr^{3+} come from the decrease of trapped electrons/holes and shortened lifetime of the electron-hole pairs. Long-lasting luminescence intensity and photocatalytic activity are highly associated. The photoluminescence properties can provide a firm foundation in theory for designing new photocatalysts with high photocatalytic activity, as well as evaluating the photocatalytic activity of some photocatalysts.

Acknowledgments

Notes and references

1   M. Allix, S. Chenu, E. V´eron, T. Poumeyrol, E. A. Kouadri-Boudjelthia, S. Alahrach´e, F. Porcher, D. Massiot and F. Fayon, *Chem. Mater.*, 2013, **25**, 1600.

2   W. N. Kim, H. L. Park and G. C. Kim, *Mater. Lett.*, 2005, **59**, 2433.

3   Y. Zhuang, J. Ueda and S. Tanabe, *Appl. Phys. Express*, 2013, **6**, 052602.

4   Q. L. M. De Chermont, C. Chanéac, J. Seguin, F. pellé, S. Maítrejean, J. P. Jolivet, D. Gourier, M. Bessodes and D. Scherman, *Proc. Natl Acad. Sci. USA*, 2007, **104**, 9266.

5   L. E. Shea, *Electrochem. Soc. Interface.*, 1998, **7** (2), 24.

6   T. Minami, Y. Kuroi, T. Miyata, H. Yamada and S. Takata, *J. Lumin.*, 1997, **72**, 997.

7   M. W. Josties, H. S. C. O'Neill, K. Bente and G. Brey, *Neues Jahrbuch fuer Mineralogie, Monatshefte*, 1995, **6**, 273.

8   A. F. Wells, *Structural Inorganic Chemistry,* Oxford University Press, London, 1975, p. 489.

9   K. Jeong, H. L. Park and S. Mho, *Solid. State. Commun.*, 1998, **105** (3), 179.

10 S. Itoh, H. Toki, Y. Sato, K. Morimoto and T. Kishino, *J. Electrochem. Soc.*, 1991, **138** (5), 1509.

11 L. E. Shea, R. K. Datta and J. J. Brown, *J. Electrochem. Soc.*, 1994, **141**, 1950.

12 P. Dhak, U. K. Gayen, S. Mishra, P. Pramanik and A. Roy, *J. Appl. Phys.*, 2009, **106** (6), 063721.

13 Ikarashi, J. Sato, H. Kobayashi, N. Saito, H. Nishiyama and Y. Inoue, *J. Phys. Chem. B*, 2002, **106**, 9048.

14 R. Zhang, A. Villanueva, H. Alamdari and S. Kaliaguine, *Catal. Commun.*, 2008, **9**, 111.

15 X. Chen, H. Xue, Z. H. Li, L. Wu, X. X. Wang and X. Z. Fu, *J. Phys. Chem. C*, 2008, **112**, 20393.

16 S. K. Sampath, D. G. Kanhere and R. Pandey, *J. Phys.: Condens. Matter.*,1999, **11** 3635.

17 H. Kawazoe and K. Ueda, *J. Am. Ceram. Soc.*, 1999, **82**, 330.

18 W. W. Zhang, J. Y. Zhang, X. A. Lan, Z. Y. Chen and T. M. Wang, *Catal. Commu.*, 2009, **10**, 1781.

19 M. Sun, D. Z. Li, W. J. Zhang, Z. X. Chen, H. J. Huang, W. J. Li, Y. H. He and X.

Z. Fu, *J. Solid. State. Chem.*, 2012, **190**, 135.

20 Q. Liu, D. Wu, Y. Zhou, H. B. Su, R. Wang, C. F. Zhang, S. C. Yan, M. Xiao and Z. G. Zou, *ASC Appl. Mater. Interfaces*, 2014, **6**, 2356.

21 S. C. Yan, J. J. Wang, H. L. Gao, N. Y. Wang, H. Yu, Z. S. Li, Y. Zhou and Z. G. Zhou, *Adv. Funct. Mater.*, 2013, **23**, 1839.

22 W. W. Zhang, J. Y. Zhang, X. A. Lan, Z. Y. Chen and T. M. Wang, *Catal. Commu.*, 2010, **11**, 1104.

23 V. B. R. Boppana and R. F. Lobo, *ACS. Catal.*, 2011, **1**, 923.

24 H. Y. Chen, L. P. Wang, J. M. Bai, J. C. Hanson, J. B. Warren, J. T. Muckerman, E. Fujita and J. A. Rodriguez, *J, Phys. Chem. C*, 2010, **114**, 1809.

25 Lkarashi, J. Sato, H. Kobayashi, N. Saito, H. Nishiyama and Y. Inoue, *J, Phys. Chem. B*, 2002, **106**, 9048.

26 Wilke and H. D. Breuer, *J. Photochem. Photobiol. A: Chem.*, 1999, **121**, 49.

27 E. Borgarello, J. Kiwi, M. Gratzel, E. Pelizzetti and M. Visca, *J. Am. Chem. Soc.*, 1982, **104**, 2996.

28 U. Scharf, H. Schneider, A. Baiker, A. Wokaun, *J. Catal.*, 1994, **145**, 464.

29 I. Litter and J. A.Navio, *J. Photochem. Photobiol. A: Chem.*, 1996, **98**, 171.

30 S. M. Karvinen, Ind. Eng. Chem. Res., 2003, **42**, 1035.

31 M. A. Butler and D. S. Ginley, *J. Electrochem. Soc.*, 1978, **125**, 228.

32 H. Nethercot, *Phys. Rev. Lett.*, 1974, **33**,1091.

33 H. Hotop and W. C. Lineberger, *J. Phys. Chem.*, 1985, **14**, 731.

34 Y. Xu and M. A. A. Schoonen, *Am. Mineral.*, 2000, **85**, 543.

35   J. Bard, R. Parsons and J. Jordan, *Standard Potentials in Aqueous Solution*, Marcel Dekker, New York, 1985.

36 Z. S. liu, X. P. Jing and L. S. Wang, *J. Electrochem. Soc.*, 2007, **154**, H 500.

37 W. N. Kim, H. L. Park and G. C. Kim, Mater. Lett., 2005, 59,2433.

38 W. Zhang, J. Zhang, X. Lan, Z. Chen and T. Wang, *Catal.Commun.*, 2010, **11**, 1104.

39 J. S. Kim, H. L. Park and C. M. Chon, *Solid. State. Commu.*, 2004, **129**, 163.

40 J. S. Kim, H. I. Kang, W. N. Kim, J. I. Kim and J. C. Choi, *Appl. Phys. Lett.*, 2003, **82** (13), 2029.

41 L. E. Shea, R. K. Datta and J. J. Brown, Jr., *J. Electrochem. Soc.*, 1994, **141**, 1950.

42 T. K. Jeong, H. L. Park and S. I. Mho, *Solid. State. Commun.*, 1998, **105**, 179.

43 Bessiere, S. Jacquart, K. Priolkar, A. Lecointre, B.Viana and D. Gourier, *Opt. Express.*, 2011, **19**, 10131.

44 J. S. Kim, J. S. Kim and H. L. Park, *Solid. State. Commun.*, 2004, **131**, 735.

45 Z. W. Pan, Y. Y. Lu and F. Liu, *Nat. Mater.*, 2012, **11**, 58.

46 R. X. Zhong, J. H. Zhang, X. Zhang, S. Z. Lu and X. J. Wang, *J. Lumin.*, 2006, **119**, 327.

47 Huang, D. Liu, C. E. Cui, L. Wang and G. Jiang, *Appl. Phys. A,* 2014, **116**, 759.

48 Y. Zhuang, J. Ueda and S. Tanabe, *J. Mater. Chem. C*, 2013, **1**, 7849.

49 S. W. S. Mckeever, *Thermoluminescence of Solids*, Cambridge University Press, Cambridge, 1985.

50 T. Matsuzawa, Y. Aoki and N. Takeuchi, *J. Electrochem. Soc.*, 1996, **143**, 2670.

51 T. Aitasalo, P. Deren, J. Hölsä, H. Jungner, J. C. Krupa, M. Lastusaari, J. Legendziewicz, J. Niittykoski and W. Strek, *J. Solid. State. Chem.*, 2003, **171**, 114.

52 H. Liu, J. Yuan, W. F. Shang-guan and Y. Teraoka, *J. Phys. Chem. C*, 2008, **112**, 8521.

53 J. Kuang and Y. Liu, *Chem. Phys. Lett.*, 2006, **424**, 58.